Chain fluctuations in the amorphous regions of polyethylene as indicated in proton relaxation spectroscopy

G. Voigt and R. Kimmich

Sektion Kernresonanzspektroskopie, Universität Ulm, Postfach 4 066, D-7900 Ulm, Federal Republic of Germany

(Received 30 January 1980)

The longitudinal relaxation of the residual protons in deuterated polyethylene has been measured with the aim to detect any heterogeneity of the amorphous methylene phase. In order to obtain a clearer distinction between 'amorphous' and 'crystalline' protons, an oxygen enhancement study has been carried out. The experiments have yielded no hint for a distribution of correlation times within the amorphous methylene phase. Therefore a single correlation function of a non-Markovian type is assumed. A model of two super-imposed defect diffusion mechanisms is suggested as an explanation for the so-called β- and γ- processes. The theoretical curves are compared with relaxation dispersion data measured in the frequency range 10^4 to 10^8 Hz by the aid of a special field-cycling apparatus.

INTRODUCTION

Partly crystalline polyethylene has been studied several times by nuclear magnetic relaxation spectroscopy[1-3]. These studies have been carried out at a single or at a few frequencies. Although the variation of temperature permitted detection of several processes of molecular motion, a full characterization was not possible because of the limited frequency range. In a preliminary report[4], we have described the first field-cycling[5] measurements of the longitudinal proton relaxation times T_1 of a solid polyethylene fraction. The available frequency range was 10^4 to 10^8 Hz, where the lower limit was given by the dipolar fields within the samples.

The relaxation data measured in refs. 1–4 are not compatible with an exponential correlation function as assumed in the BPP formula[6] frequently used in its unmodified form in the literature. There are two possibilities to understand the discrepancies: either the correlation function is in reality non-exponential, i.e. the relevant processes of molecular motion are non-Markovian[7], or a distribution of (exponential) correlation functions exists[8]. The latter explanation implies a structural inhomogeneity within the sample, so that different protons obey different fluctuations within the time scale of the relaxation times or longer.

Structural heterogeneities can be found in partly crystalline polyethylene samples at least with respect to amorphous and crystalline regions or methylene and methyl groups. However, the influence of the end groups is certainly negligible at temperatures above the glass point and for longer polymer chains. The proportionality of the rate T_1^{-1} to the amorphous content[3,9], on the other hand, shows that the amorphous regions dominate the total relaxation. Thus the question must be discussed, whether the amorphous regions have to be considered as a homogeneous phase above the glass transition in a time scale of T_1.

As an experimental approach to solve this problem, we report investigations of the enhancement of the relaxation rate by dissolved oxygen. The conclusion is, that the amorphous regions relax homogeneously above the glass transition, so that a single non-exponential correlation function has to be used for the description of the frequency and temperature dependence of T_1. As a non-Markovian motion, we discuss the re-orientation of segments by diffusing defects (e.g. $gt\bar{g}$-sequences, torsions). Several models of this type have been treated and reviewed previously[7].

EXPERIMENTAL

Above 20 MHz, we have measured T_1 by the 90°/90°-pulse method using a conventional pulse spectrometer (Bruker SXP 4 - 100). In the low-frequency range (2×10^4 to 2×10^7 Hz), a special field-cycling spectrometer has been used[10]. This apparatus consists of a pulsed power supply, a cryomagnet and a conventional RF equipment.

In order to achieve the RF bandwidth necessary for solid state investigations, detection frequencies well above 10^7 Hz are required. This means, that a high power has to be supplied to a small magnet coil. The problems arising thereof concern the cooling of the magnet and the fast and precise regulation of the current.

Two different magnet coils have been provided. First, a copper coil has been used which is cooled in a bath of liquid nitrogen, so that the ohmic resistance is only about 15% of the value at room temperature. The dimensions of the coil have been calculated with the Garrett–Loney formalism[11,12]. A cross-section is given in *Figure* 1. The maximum magnetic flux density in steady-state operation is 0.47 T (corresponding to 20 MHz proton resonance frequency).

The second magnet coil was wound with Nb–Ti multifilament superconductors (Intermagnetics) producing pulsed flux-densities up to 1.2 T (corresponding to 50 MHz proton resonance frequency). Both coils have an inductance of less than 100 mH and an unshimmed

0032-3861/80/091001-08$02.00

homogeneity of better than 5×10^{-5} within the sample volume (about 1 cm^3). For the present applications, it turned out that the sensitivity attainable with the copper coil was sufficient, so that all field-cycling data reported in this paper have been measured with this coil.

The pulsed power supply (Tekelec-Airtronic) provides a maximum output current of 60 A and a peak voltage of 350 V (during the raising period). The stability is better than 5×10^{-5} for the detection field (>0.5 T) and better than 10^{-2} for a relaxation field of 10^{-3} T. A field stable enough for the signal detection is reached within 30 ms. Starting from zero, a flux density of 0.1 T is passed within 4 ms with the copper coil and within 2 ms with the superconducting solenoid. The course of the field rise is precisely reproducible, so that no corrections for the switching periods are necessary[13]. T_1 values down to 5 ms can thus be measured provided that there is a sufficient field dependence of T_1.

The probe head is arranged in a glass Dewar in the magnet coil. The sample volume is 1 cm^3. The interior of the probehead Dewar has been evacuated during the measurements of the diamagnetic relaxation times in order to remove any oxygen. All longitudinal relaxation curves except those of the perdeuterated samples were found to be exponential.

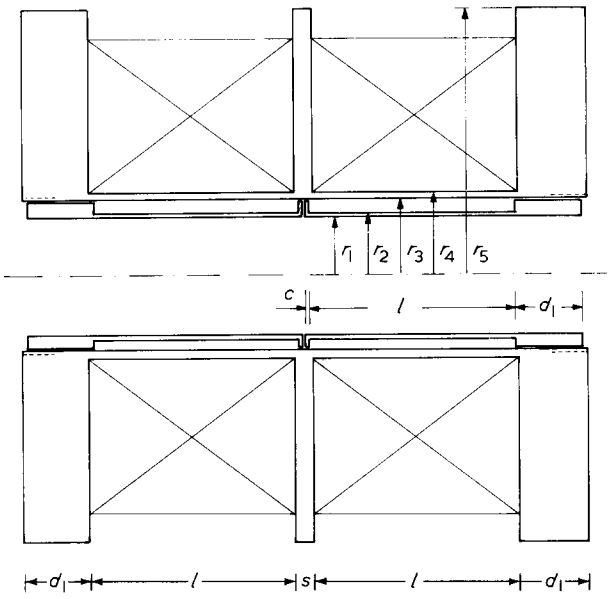

Figure 1 Cross-section of the nitrogen cooled copper coil. The dimensions are:
r_1 = 17.5 mm, r_2 = 18.5 mm, r_3 = 22.5 mm,
r_4 = 24.5 mm, r_5 = 80.0 mm, C = 1.0 mm,
s = 4.4 mm, d_1 = 19.5 mm, l = 63.5 mm.
The main coil-former was made of aluminium and was slit and perforated. Optionally concentric correction coils can be used. The coil-formers thereof were made of Durcoton (Felton & Guillaume, Köln). The main coil was wound of rectangular wires (2.25 x 1.25 mm^2). Spacing mats of glass fibre have been used

Table 1 characterizes the fractions of linear polyethylene used in this paper. Most of the crystallinities have been calculated from the densities obtained by the aid of the suspension method[14]. The densities for pure amorphous and pure crystalline material have been taken from ref. 15.

The oxygen enhanced relaxation rates have been measured as described previously[16].

HOMOGENEITY OF THE AMORPHOUS PHASE

The effective longitudinal relaxation of partly crystalline polyethylene is dominated by the methylene group motions in the amorphous regions[9] at medium temperatures (200 K$\lesssim$T$\lesssim$320 K). Below this range, the rotational diffusion of methyl end groups becomes relevant[3], while at higher temperatures the influence of the so-called α-process of the crystallites is no more negligible[17]. The averageing mechanism between these proton phases is caused by spin diffusion[6]. An important question for the discussion following below is now, whether the methylene groups in the amorphous phase relax homogeneously or whether there is a distribution of correlation times.

The relaxation curves themselves can give the answer provided there is a way to interrupt the spin diffusion mechanism, so that any distribution of correlation times is revealed by a distribution of relaxation times. In other words, we have to investigate a sample with isolated proton groups as provided, e.g. by the residual protons of a highly deuterated sample. The specially synthesized polyethylene used for this purpose has been specified by the producer to consist of 98% —$[C_2D_4]$— and 2% randomly distributed —$[C_2H_4]$— groups. The longitudinal proton relaxation curves thus should be composed of at least two exponentials according to the crystalline and amorphous regions.

The data observed at room temperature were found to be clearly non-exponential (*Figure* 2) and could be analysed into two as well as into three exponential functions[18]. A further problem in the interpretation of these data is that the absence of 'mixed' groups such as —$[C_2H_2D_2]$— or —$[C_2HD_3]$— was claimed by the producer but could not be controlled in our laboratory.

To overcome these difficulties, an experimental situation is required, where the proton–proton interaction can be separated and where the relaxation times of the amorphous and the crystalline regions are so different from each other that an unambiguous analysis becomes possible. Empirically this difference should be about one order of magnitude or more.

We have therefore carried out a relaxation enhancement experiment by applying an oxygen pressure of 50 bar on the sample. Oxygen is electron paramagnetic so that the additional dipolar interaction, which the protons

Table 1 Characterization of the samples (M_W = weight-average molecular weight, M_n = number average molecular weight, ρ = density at 20°C)

	Sample	M_W	M_W/M_n	ρ (g/cm^3)	Crystallinity (%)	Supplier
1	$[C_2H_4]_n$	2482	1.11	0.975	86	Polymer Lab. (RAPRA), Shrewsbury, UK
2	$[C_2H_4]_n$	20400	1.10	0.957	74	Knauer, West Berlin
3	$[C_2H_4]_n$	92300	1.10	0.935	59	Knauer, West Berlin
4	$[C_2H_4]_n$	675000	1.18	0.958	74	Knauer, West Berlin
5	2% $[C_2H_4]$ in 98% $[C_2D_4]_n$				76 (X-ray)	Merck, Sharp, Dohme, Kirkland, Canada

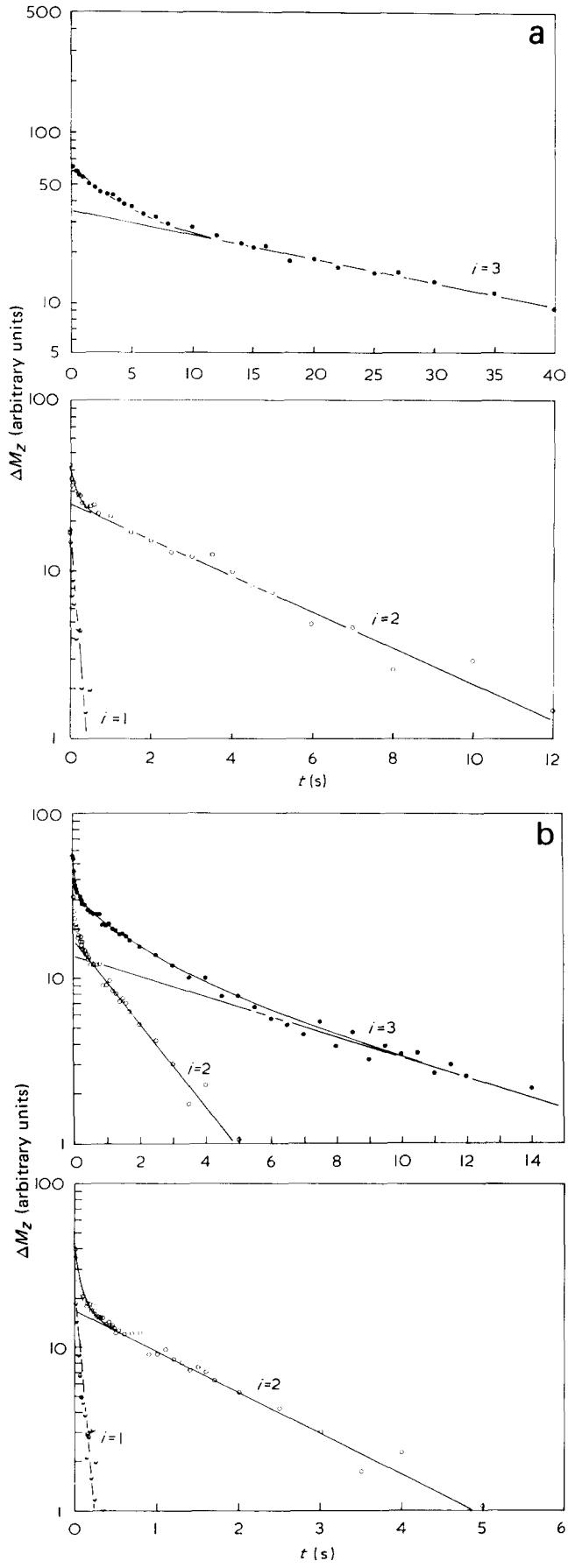

Figure 2 Longitudinal relaxation curves measured with the deuterated sample (98% $+C_2D_4+$, 2% $+C_2H_4+$) before and after application of an oxygen partial pressure of 50 bar.. The frequency was 90 MHz. 20 signal pairs were accumulated for each data point. Oxygen enhanced: (a) 243 K, (b) 300 K. Diamagnetic: (c) 297 K. The parameters of the analysis are given in *Table 2*

experience, causes a reduction of the relaxation according to the local oxygen concentration. This enhancement will be selective, as the amorphous and crystalline regions show quite different solubilities of oxygen[19,20]. Practically there is no detectable solubility in the crystallites, so that the influence of oxygen clearly separates 'crystalline' and 'amorphous' components.

Before discussing the results of this experiment, it should be clarified which correlation time dominates the proton–oxygen interaction. As the electron spin relaxation time τ_s is extremely short in the case of oxygen, it was argued[21] that the effective correlation time in aqueous solutions should be equal to τ_s. The same argument holds for oxygen dissolved in alkane phases[20]. The electron spin relaxation time τ_s is virtually insensitive to the structural environment. Constant τ_s-values at the various phase transitions of paraffins have been found[22]. The oxygen–proton interaction is therefore not affected by any change of the proton mobility.

The local oxygen solubility depends on the available free volume[22], which, on the other hand, determines the segment mobility[23]. Thus, the relaxation enhancement is indirectly connected with the mobility of the 'amorphous' chain segments.

Figure 2 shows the experimental results and the analysis into three components. The T_1-values are given in *Table* 2. The long and the medium component are attributed to the crystalline regions. No relaxation enhancement by oxygen can be detected and the sum of their amplitudes corresponds well to the crystallinity (*Table* 1). Furthermore the T_1 values of these components are too long for a considerable contribution to the total relaxation in the undeuterated case. An interpretation of these two 'crystalline' components is difficult. Either they reflect ethylene groups with a different degree of deuteration or with different mobility (e.g. in the surface layer of the crystallites). The first interpretation, however, contradicts the specification given by the supplier of the deuterated polyethylene.

The remaining short component must be attributed to the amorphous regions. It is strongly affected by dissolved oxygen, its amplitude corresponds to the amorphous content and its diamagnetic T_1 value is short enough to relax the whole sample in the undeuterated case as discussed above. As there is no deviation from an exponential decay within the experimental error, we have to deal with a virtually homogeneously relaxing phase. This means that the local free volume averaged over the relaxation times must be homogeneously distributed, so that there is no indication for a broad distribution of correlation times in the parts of the sample which dissolve

oxygen. In the following we will therefore assume a single correlation function of the non-Markovian type.

The components discussed in this section are not necessarily identical to the three components discussed with wide-line spectra[9,24]. A difference may arise from the fact that the line-width is mainly affected by the slowest of several (anisotropic) processes a segment suffers, while the diamagnetic contribution to the longitudinal relaxation is dominated by fluctuations near the Larmor frequency. The paramagnetic contribution, on the other hand, depends on the local oxygen concentration, i.e. the free volume. Thus, the line width and the longitudinal relaxation of a definite phase may be dominated by different mechanisms. Merely the division into 'crystalline' and 'amorphous' regions is certainly comparable in both methods. This can clearly be verified by comparing transverse and longitudinal relaxation data[39].

Table 2 Parameters of the longitudinal relaxation curves obtained with sample no. 5 before and after application of an oxygen partial pressure of 50 bar (*Figure 2*). The curves have been fitted according to $\Delta M_z(t) = \Delta M_z(0)\ \Sigma_{i=1}^{3}\ a_i\ e^{-t/T_1^{(i)}}$ (ΔM_z is the deviation of the z-magnetization from the equilibrium value)

	Oxygen enhanced				Diamagnetic (297 K)	
	243 K		300 K			
i	$T_1^{(i)}$ (s)	a_i	$T_1^{(i)}$ (s)	a_i	$T_1^{(i)}$ (s)	a_i
1 ('short')	0.15	0.22	0.07	0.25	0.4	0.17
2 ('medium')	4.0	0.33	1.7	0.31	1.4	0.37
3 ('long')	31.5	0.45	7.1	0.44	7.5	0.46

DEFECT DIFFUSION MODELS

As suitable non-Markovian correlation functions we suggest those of the class of defect diffusion models. We will mainly refer to the two-state models treated in ref. 7 for defects with 'restoring capability'. This means that the initial interaction state is restored after the passage of the defect. Thus our discussion mainly concerns defects such as kinks or local torsions diffusing up and down the chains. The resulting formulae are given in *Table* 3. We

Table 3 Intensity and correlation functions for defect diffusion models. The symbols are defined as follows: τ_b, diffusion time over the width b of a defect; τ_a, diffusion time over the diameter a of a defect; $\tau_l = \pi l_0^2\ (16\ D)^{-1}$; $2l_0$, mean distance from defect to defect; D, defect diffusion coefficient; τ_d, diffusion time over the distance d from reflecting barrier to reflecting barrier; erf (. . .) error function; C_2 and S_2, Fresnel integrals

Model	Normalized correlation function $G_n(\tau)$	Intensity function $J_n(\omega)$	Ref.
Defects with restoring capability; unlimited diffusion in one dimension	$\mathrm{erf}\left(\sqrt{\frac{\tau_b}{2\tau}}\right) - \sqrt{\frac{2\tau}{\pi\tau_b}}\,[1-\exp(-\tau_b/2\tau]$	$\tau_b^{-1/2}\,\omega^{-3/2}\,\{1-\exp(-\sqrt{\omega\tau_b})\,[\cos\sqrt{\omega\tau_b}+\sin\sqrt{\omega\tau_b}\,]\}$	7
Defects without restoring capability; unlimited diffusion in one dimension	$\exp\left(-\sqrt{\frac{\tau}{\tau_l}}\right)$	$\sqrt{\frac{2\pi}{\tau_l}}\,\omega^{-3/2}\,\{\cos(\alpha)\,[\frac{1}{2}-C_2(\alpha)]+\sin(\alpha)\,[\frac{1}{2}-S_2(\alpha)]\}$ with $\alpha=(4\omega\tau_l)^{-1}$	7, 29
Defects with restoring capability; diffusion in one dimension limited by two reflecting barriers	lengthy expression	$\omega\tau_d \ll 1$: $\frac{2}{3}\tau_b\left(\sqrt{\frac{\tau_d}{\tau_b}}-1\right)$ $\omega\tau_b \ll 1 \ll \omega\tau_d$: $\sqrt{\tau_b\tau_d}\,\frac{\sqrt{\tau_d}-2\sqrt{\tau_b}}{(\sqrt{\tau_d}-\sqrt{\tau_b})^2}\,\frac{1}{\omega^{1/2}}$ $\omega\tau_b \gg 1$: $\sqrt{\frac{\tau_d}{\tau_b}}\left(\frac{1}{\omega^{3/2}\,\tau_b^{1/2}\left(\sqrt{\frac{\tau_d}{\tau_b}}-1\right)}-\frac{3}{4\omega^2\,\tau_b\left(\sqrt{\frac{\tau_d}{\tau_b}}-1\right)^2}\right)$	10, 37, 38
Defects with restoring capability; unlimited diffusion in three dimensions	$\tau = 0$: 1 $\tau > 0$: $\frac{1}{2}\,\mathrm{erf}\left(\sqrt{\frac{3\tau_a}{2\tau}}\right)\sqrt{\frac{2\tau}{3\pi\tau_a}}\left[1-\exp\left(-\frac{3\tau_a}{2\tau}\right)\right]$	$(3\tau_a)^{-1/2}\,\omega^{-3/2}\,[1-\exp(-\sqrt{3\omega\tau_a})\,(\cos\sqrt{3\omega\tau_a}+\sin\sqrt{3\omega\tau_a}\,\{1+\sqrt{3\omega\tau_a}\})]$	7

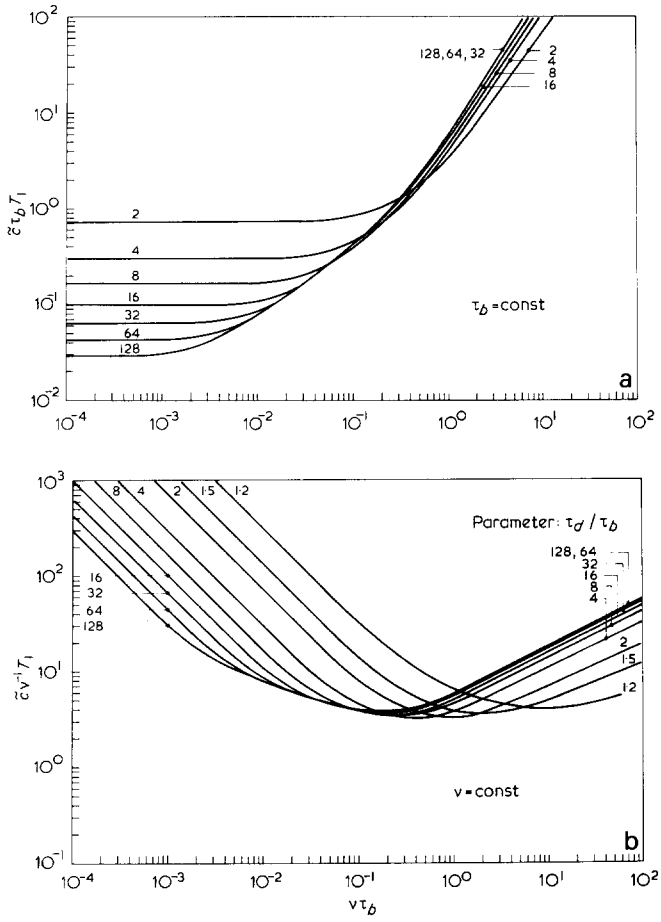

Figure 3 Limited diffusion in one dimension of defects with restoring capability (*Table 3*): Theoretical behaviour of T_1 as a function of (a) the frequency ν and (b) the diffusion time τ_b. The curve parameter is the ratio τ_d:τ_b. Further quantities are:

$$\tilde{C} = \frac{9}{8}\gamma^4\hbar^2\sigma^{(1)}\left(\frac{\mu_0}{4\pi}\right)^2,$$

where γ is the magnetogyric ratio and

$$\sigma^{(1)} = \langle|F^{(1)}|^2\rangle - |\langle F^{(1)}\rangle|^2,$$

$$F^{(1)} = R^{-3}\cos\theta\sin\theta\exp(-i\Phi).$$

R, θ, Φ are the spherical coordinates of the distance vector between two spins

distinguish unlimited one- or three-dimensional and limited one-dimensional defect diffusion.

The latter concerns defects which are assumed to be reflected either at each other or at structural barriers (e.g. chain folds or crystallites). The distance between these barriers is designated by d, the width of a defect by b. We have then two important diffusion times, namely

$$\tau_d = \frac{d^2}{2D} \quad \text{and} \quad \tau_b = \frac{b^2}{2D} \qquad (1)$$

where D is the defect diffusion coefficient. The limiting formulae reported in our previous paper[7] hold for ratios τ_d:$\tau_b \gg 1$. In order to generalize these expressions, we have carried out approximations up to the sixth order leading to formulae valid for all ratios τ_d:$\tau_b > 1$. Graphical representations are given in *Figures* 3 and 4. *Figure* 4 shows the value of $(\omega\tau_b)_{min}$ at the T_1 minimum as a function of τ_d:τ_b.

The non-Markovian correlation functions given in *Table* 3 have to be considered in comparison with formal distributions of correlation times. Such distributions have first been introduced for the interpretation especially of dielectric relaxation data[26] and have been discussed by the aid of the so-called Cole–Cole plot. This is a common method to show the deviations from an exponential correlation function (Debye model). In *Figure* 5, we show

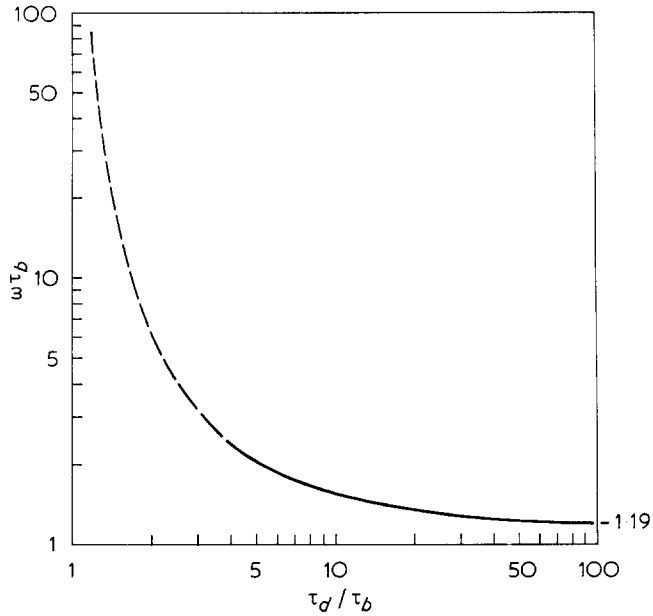

Figure 4 Conditions $\omega\tau_b = x$ for the T_1-minimum as a function of τ_d:τ_b for limited defect diffusion in one dimension (*Table 3*). The broken part of the curve holds reservedly because here assumptions of the model become critical[37]

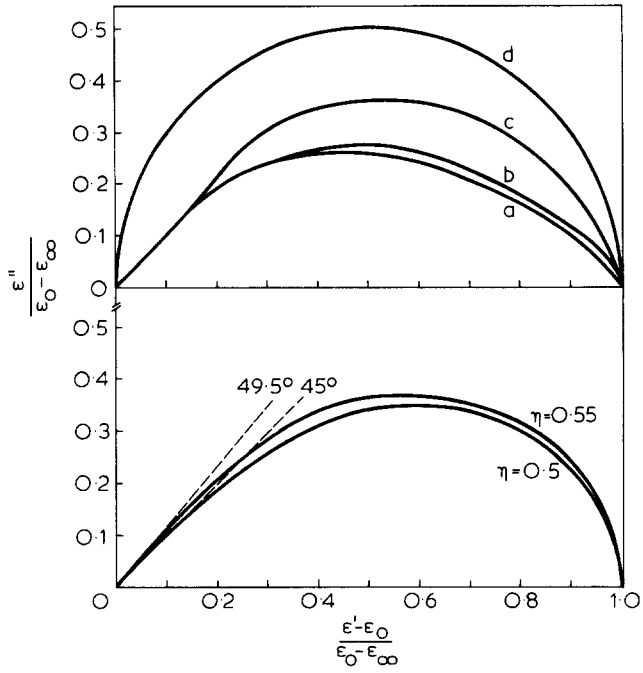

Figure 5 Cole–Cole plots for the various mechanisms. Upper: diffusion of defects with restoring capability (a) in one dimension without limitation; (b) in one dimension with limitation (τ_d/τ_b = 100); (c) in three dimensions without limitation; (d) Debye model. Lower: Cole–Davidson distribution:

$$\frac{\epsilon' - \epsilon_\infty}{\epsilon_0 - \epsilon_\infty} = (\cos\phi)^\eta \cos\eta\phi$$

$$\frac{\epsilon''}{\epsilon_0 - \epsilon_\infty} = (\cos\phi)^\eta \sin\eta\phi$$

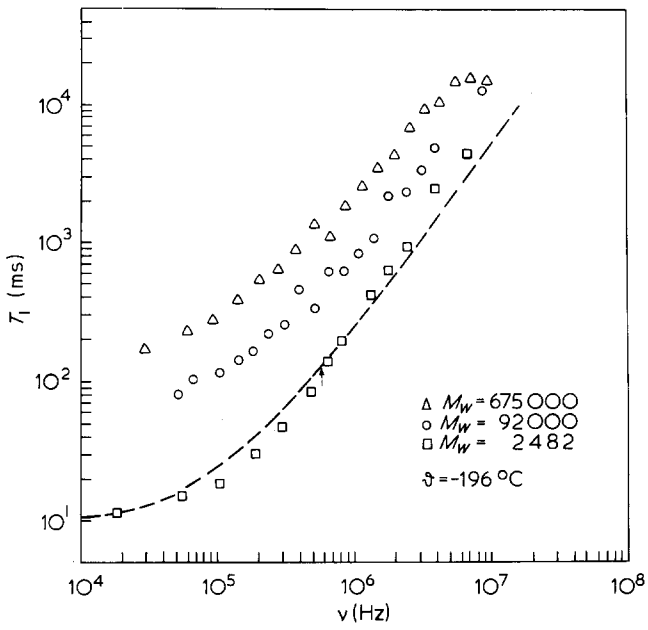

Figure 6 T_1 dispersion of three fractions of linear polyethylene at nitrogen temperature. The data for the short chain fraction are strongly influenced by methyl group rotation (compare *Figure 7*). The broken line has been calculated for unlimited diffusion of defects without restoring capability (*Table 3*). The arrow indicates the position $\omega\tau_I = 1$. Fits of the same quality can be achieved with a Cole–Davidson distribution of correlation times or with the model for three-dimensional diffusion of defects with restoring capability

the comparison between the diverse defect diffusion models with the Cole–Davidson distribution[27,28] and the Debye model. There is a strong similarity between the skewed arcs obtained for a Cole–Davidson distribution and for three-dimensional diffusion of defects with restoring capability, and also for one-dimensional diffusion of defects without restoring capability[7,29].

In the following we have to deal with the case that more than one 'process' determine the molecular fluctuations. This means that an effective correlation function $G(\tau)$ and from this the effective intensity function $J(\omega)$ has to be derived from the functions holding for the individual processes alone.

We assume that the amorphous methylene groups are influenced by two independent processes designated by β and γ. The individual correlation functions are $G_\beta(\tau)$ and $G_\gamma(\tau)$. These functions don't decay to zero as we consider anisotropic motions. For the effective correlation function we use the relation

$$G(\tau) = G_\beta(\tau)G_\gamma(\tau) \tag{2}$$

$G_\gamma(\tau)$ can be analysed according to $G_\gamma(\tau) = \tilde{G}_\gamma(\tau) + G_\gamma^\infty$ where $G_\gamma^\infty = G_\gamma(\tau \to \infty)$ and $\tilde{G}_\gamma(\tau \to \infty) = 0$. Assuming now that these two processes occur in completely different time scales, so that $G_\gamma(\tau)$ has already decayed to its final value $G_\gamma^\infty = G_\gamma(\tau \to \infty)$ before $G_\beta(\tau)$ perceptibly deviates from its initial value G_β^0, leads to the approximation

$$G(\tau) = (\tilde{G}_\gamma(\tau) + G_\gamma^\infty)G_\beta(\tau) \approx \tilde{G}_\gamma(\tau)G_\beta^0 + G_\beta(\tau)G_\gamma^\infty \tag{3}$$

The intensity function is then given by the weighted sum of the functions for the individual processes.

$$J(\omega) = G_\beta^0 J_\gamma(\omega) + G_\gamma^\infty J_\beta(\omega) \tag{4}$$

Therefore we have simply to form the weighted sum of the relaxation rates expected for the individual processes in order to obtain the effective relaxation rate.

DISCUSSION OF THE T_1 DISPERSION

Starting from nitrogen temperature, the first process which becomes visible in the available frequency range is attributed to methyl end-group rotation (*Figure* 6). As we have investigated linear polyethylene, there is a strict relation between the chain length and the concentration X_m of the methyl groups:

$$\frac{1}{T_1} = \frac{X_m}{T_1^{CH_3}} + \frac{\alpha(1-X_m)}{T_1^{CH_2,\alpha}} \tag{5}$$

where α is the amorphous fraction, $T_1^{CH_3}$ the relaxation time of the methyl groups and $T_1^{CH_2,\alpha}$ that of the 'amorphous' methylene groups. (The contribution of the crystalline regions can be neglected at nitrogen temperature.) Equation (5) fits well the results obtained with different chain lengths (*Figure* 7, compare also ref. 3), so that there is no doubt about the origin of this process. Less clear is the type of correlation function relevant for methyl group rotation in amorphous materials. The frequency dependence of T_1 for PE 2 482 at nitrogen temperature which is dominated by this process can be described well by one-dimensional diffusion of defects without restoring capability (*Table* 3). If that model were true, the methyl group rotation would be initiated for example by diffusing vacancies lowering the local density and therefore the inter-chain restriction.

On the other hand, this curve can be fitted by a Cole–Davidson distribution of correlation times in agreement with the finding for polypropylene[30]. As the arguments of

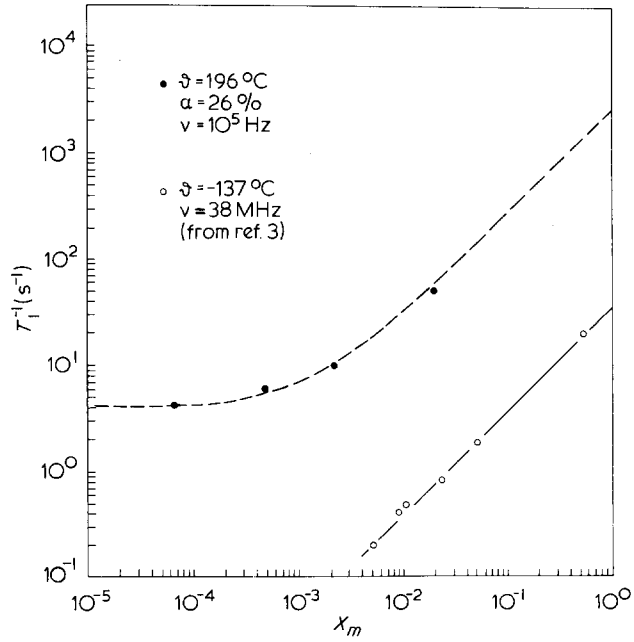

Figure 7 Longitudinal relaxation rates *versus* the fraction of methyl protons. The broken line has been fitted according to equation (5) after correcting all data points for an amorphous content α = 26%. The parameters are $T_1^{CH_2,\alpha} = 0.25$ s and $T_1^{CH_3} = 0.37$ ms at −196°C and 10^5 Hz. Data for branched polyethylene and polypropylene (x_m = 0.5) are also presented for comparison[3]

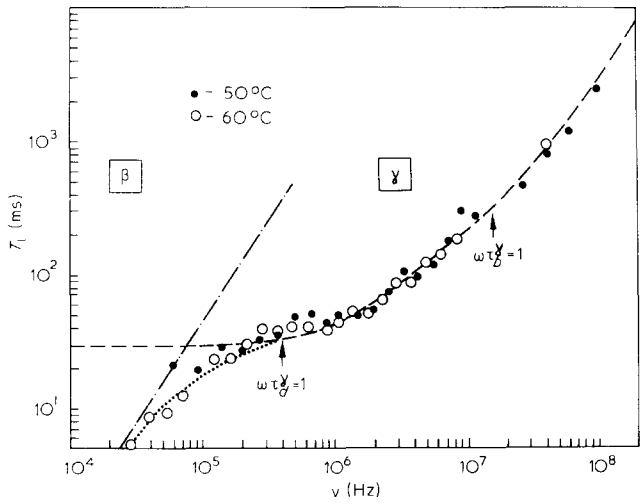

Figure 8 T_1 dispersion of linear polyethylene $M_W = 675\,000$ at −50°C and −60°C (γ-process). The broken line has been calculated for limited diffusion of defects with restoring capability (*Table 3*). The parameters are given in *Table 4*. The theoretical curve in *Figure 9* has been calculated with the same parameters

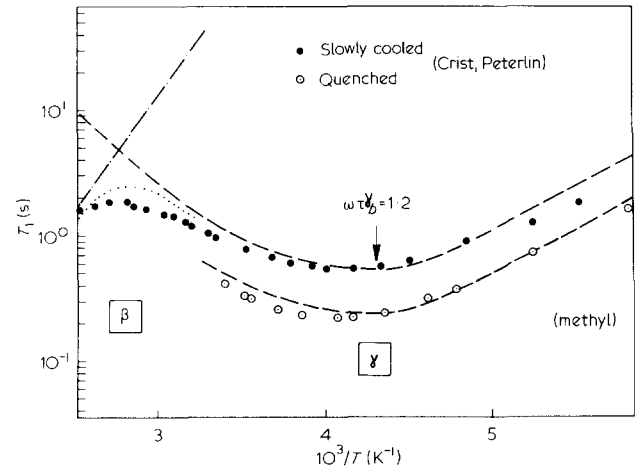

Figure 9 Temperature dependence of T_1 for linear polyethylene at 38 MHz. (Experimental data from ref. 3.) The minima indicate the γ-process. The broken lines have been calculated for limited diffusion of defects with restoring capability (*Table 3*).. The parameters are in coincidence with those used in *Figure 8* (*Table 4*). At the highest temperatures the influence of the β-process becomes visible. The overlap region is indicated by . . . . .

the section on homogeneity concern exclusively the amorphous methylene groups, we have no possibility for a distinction. (An oxygen enhancement experiment could not be carried out because no partly deuterated material of this molecular weight is available.) We can merely draw the attention to a discrepancy arising with the assumption of the Cole–Davidson distribution. This distribution of correlation times can be interpreted as a distribution of apparent activation energies caused by the inter-chain interactions. In other words, all apparent activation energies *less* than a certain amount E_m contribute. The value fitted for E_m was found to be 12.1 kJ/mol for amorphous polymers[30]. The activation energy found or calculated for the intra-chain potentials of paraffins is 14.2 kJ/mol [31–34]. So the distribution is extended to the wrong side of this value, leaving no space for inter-chain interactions. This difficulty would be overcome by the assumption of a single correlation function, e.g. of the type mentioned above. As we have no direct experimental hint for such a model, we content ourselves with this qualitative statement.

Figures 8 and 9 show the T_1 dispersion at −50°C and the temperature dependence of T_1. These curves are dominated by the so-called γ-process. Both sets of data can be described by the model for the limited diffusion of defects with restoring capability. (The absolute values of the T_1 data in *Figures* 8 and 9 are shifted to each other according to the different crystallinities of the samples.) The parameters given in *Table* 4 are in agreement with other investigations reported in the literature[2,41].

The slight deviation of the theoretical curve from the experimental data at the high-temperature side of the minimum in *Figure* 9 can be explained by an additional temperature dependence of the parameters which has not yet been assumed. For instance it might be possible that the amplitude of the chain fluctuations is increased with the temperature as a consequence of the larger free volume. A corresponding conclusion has been drawn from a deuterium line-shape analysis[40].

The assumption that the defects causing the γ process are virtually kinks ($gt\bar{g}$-sequences) fits the activation energy expected for kink steps[34]. The distance from equilibrium position to equilibrium position of a kink is equal to the projection of two CH_2 groups on the chain axis (i.e. 2.54 Å). Assuming that this distance is equal to the defect width b leads, together with the ratio $\tau_d^\gamma:\tau_b^\gamma = d_\gamma^2:b_\gamma^2 \approx 40$, to an average distance equal to the projection of 13 CH_2 groups on the chain axis or $d_\gamma = 16.1$ Å. Assuming further that the reflecting barriers are the nearest neighbour kinks of a reference defect, means that the defect concentration is about 16% (1 kink per 6 methylene groups), i.e. a value which is not unreasonable in the light of second moment values of the amorphous regions[25].

The next process becomes visible in our frequency range at about 30°C (*Figure* 10). It is designated by the letter β. A description by the model for limited diffusion of defects is again possible. This means that there is a second type of defects diffusing *independently* of the kink defects causing the γ process. A potential distortion of this type is chain torsions. In this case we have to consider the crystallite surfaces, where the amorphous chains are anchored, as reflecting barriers. The time parameters are then τ_d^β and τ_b^β. For a definite temperature it holds $\tau_{d,b}^\beta \gg \tau_{d,b}^\gamma$, so that the approximative formula (4) can be used. *Figure* 10 shows beside the theoretical curve for the β process alone the effective T_1-dispersion in the overlap region with the γ process. The parameters of this process are given in *Table* 4.

Formally the same description can be obtained with a somewhat different view of the β-process. It is irrelevant whether a defect diffuses towards the segment referred to or vice versa. The latter case means that the amorphous chain parts are assumed to diffuse longitudinally forth and back within a certain range. A reference segment is then carried by the diffusing chain around conformational

Table 4 Parameters used for the description of the T_1 data in the temperature/frequency range of the β- and γ-process. The quantities are defined by the Arrhenius law: $\tau_b = \tau_b^\infty \exp(E/RT)$

Process	τ_b^∞ / s	E (kJ/mol)	$\tau_d:\tau_b$
β	5.2×10^{-21}	71.6	10^2
γ	3.3×10^{-15}	27.8	40

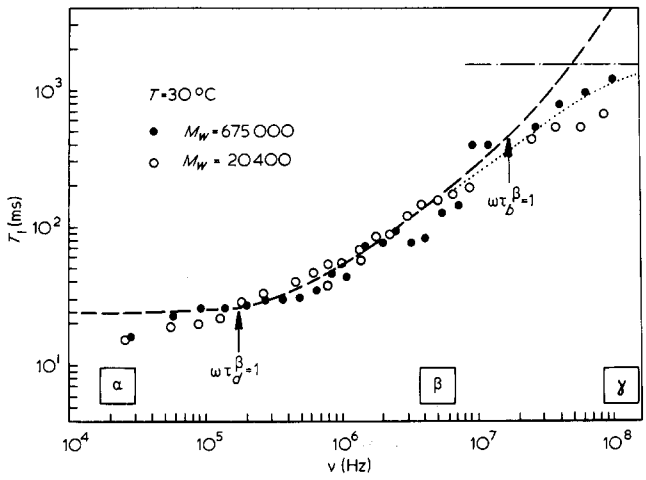

Figure 10 T_1 dispersion of linear polyethylene M_W = 675 000 and M_W = 20 400 at 30°C (β-process). The broken line has been calculated for limited diffusion of defects with restoring capability (*Table 3*). With the parameters for the β-process given in *Table 4* and the extrapolated relaxation rate of the γ-process the overlap region of both processes could be described according to equation (4) (. . .). Below 10^5 Hz the influence of the so-called α-process of the crystallites becomes visible

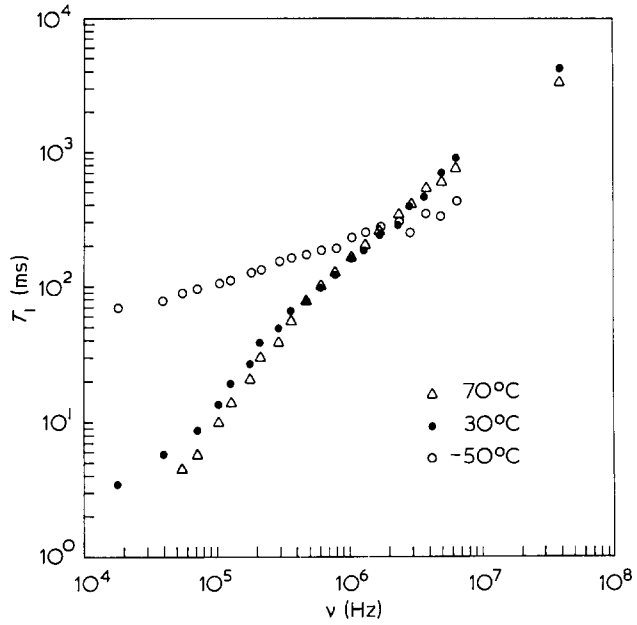

Figure 11 T_1-dispersion of linear polyethylene M_W = 2482 at −50°C 30°C and 70°C

bends so that the segment orientation is altered. In other words we have then to replace the term 'defect' by 'chain bend' and 'limited defect diffusion' by 'limited longitudinal chain diffusion' (or 'limited reptation'). The chain-bends are fixed by the local microstructure, so that it can be assumed that the amorphous chain parts have only a (limited) degree of freedom in longitudinal direction.

A quite different behaviour is shown by sample 1 (molecular weight $M_w = 2482$, crystallinity 86%). No clear T_1 dispersion regions attributable to the γ or β process could be detected (*Figure* 11). These findings coincide with the observation that this fraction shows X-ray patterns similar to those of crystalline paraffins[35]. A molecular weight dependence of the n.m.r. wide-line components has been found by Kitamaru *et al.*[36]. Clearly there is no comparable amorphous phase at the low molecular weights.

The T_1 dispersion shown in *Figure* 11 at low frequencies for 30 or 70°C must be attributed to the so-called α-process of the crystalline regions. Models for this type of motion are reported in refs. 15 and 17.

The essential result of the presented analysis is that there are defects diffusing in a very restricted manner along the chains. A similar conclusion has been drawn[40] from a computer simulation of the deuterium line-shape of polyethylene. It has been concluded that the kink diffusion is restricted to rather short chain parts irrespective of the distance of the fixed ends of the chain. The same behaviour can be expected from the picture outlined in this paper.

ACKNOWLEDGEMENTS

This work has been supported by Deutsche Forschungsgemeinschaft. Thanks are due to Dr B. Heise, Universität Ulm, for kindly determining the crystalline content of one sample.

REFERENCES

1 Trappeniers, N. J., Gerritsma, C. J. and Oosting, P. H. *Physica* 1964, **30**, 997
2 Haeberlen, U. *Kolloid-Z. Z. Polym.* 1968, **225**, 15
3 Crist, B. and Peterlin, A. *J. Macromol. Sci. (Phys.)* 1970, **B4**, 791
4 Voigt, G. and Kimmich, R. *Chem. Phys. Lett.* 1978, **56**, 275
5 Kimmich, R. *Bull. Magn. Resonance*, in press
6 Abragam, A. 'The Principles of Nuclear Magnetism', Oxford University Press, Oxford, 1961, p 300
7 Kimmich, R. and Voigt, G. *Z. Naturforsch.* 1978, **33a**, 1294
8 Connor, T. M. *Trans. Faraday Soc.* 1964, **60**, 1574
9 Bergmann, K. and Nawotki, K. *Kolloid.-Z. Z. Polym.* 1967, **219**, 132
10 Voigt, G. *Thesis*, Universität Ulm (1979)
11 Garrett, M. W. *J. Appl. Phys.* 1951, **22**, 1091
12 Loney, S. T. *J. Inst. Math. Appl.* 1966, **2**, 111
13 Voigt, G. and Kimmich, R. *Progr. Colloid Polym. Sci.* 1979, **66**, 273
14 Elias, H.-G. 'Makromoleküle', Hüthig & Wepf, Heidelberg, 1975
15 Ashcraft, C. R. and Boyd, R. H. *J. Polym. Sci. (Polym. Phys. Edn)* 1976, **14**, 2153
16 Peters, A. and Kimmich, R. *Biophys. Struct. Mechanism* 1978, **4**, 67
17 Olf, H. G. and Peterlin, A. *J. Polym. Sci. (A2)* 1970, **8**, 771
18 Douglass, D. C., McBrierty, V. J. and Weber, T. A. *Macromolecules* 1977, **10**, 178
19 Michaels, A. S. and Bixler, H. J. *J. Polym. Sci.* 1961, **50**, 393
20 Kimmich, R. and Peters, A. *Chem. Phys. Lipids* 1975, **14**, 350
21 Hausser, R. and Noack, F. *Z. Naturforsch.* 1965, **20a**, 1668
22 Peters, A. *Thesis*, Universität Ulm (1979)
23 Cohen, M. H. and Turnbull, D. *J. Chem. Phys.* 1959, **31**, 1164
24 McBrierty, V. J. *Faraday Discuss. Chem. Soc.* 1979, **68**, in press
25 Schmauder, Kh. *Diplomarbeit*, Universität Ulm (1976)
26 Hill, R. M. *Nature* 1978, **275**, 96
27 Davidson, D. W. and Cole, R. H. *J. Chem. Phys.* 1950, **18**, 1417
28 Davidson, D. W. and Cole, R. H. *J. Chem. Phys.* 1951, **19**, 1484
29 Bordewijk, P. *Chem. Phys. Lett.* 1975, **32**, 592
30 Kienzle, U., Noack, F. and Schütz, J. V. *Kolloid.-Z. Z. Polym.* 1970, **236**, 129
31 Hoyland, J. R. *J. Chem. Phys*, 1968, **49**, 1908
32 Grant, R. M. *et al.*, *J. Chem. Phys.* 1970, **52**, 4424
33 Pitzer, K. S. *J. Chem. Phys*, 1937, **5**, 473
34 Hägele, P. C. and Pechhold, W. *Kolloid-Z. Z. Polym.* 1970, **241**, 977
35 Wilke, W. and Asbach, I. personal communication
35 Kitamaru, R., Horii, R. and Hyon, S.-H. *J. Polym. Sci. (Polym. Phys. Edn)* 1977, **15**, 821
37 Kimmich, R. *Z. Naturforsch.* 1976, **31a**, 693
38 Kimmich, R. and Peters, A. *J. Magn. Resonance* 1975, **19**, 144
39 Fedotov, V. D. and Abdrashitova, N. A. in 'Magnetic Resonance and Related Phenomena', (Eds. E. Kundla, E. Lippmaa, T. Saluvere), Springer-Verlag, Berlin, 1979
40 Rosenke, K., Sillescu, H. and Spiess, H. W. in press
41 Pechhold, W. and Blasenbrey, S. *Agnew. Makromol. Chem.* 1972, **22**, 3